JOURNAL OF COMPUTATIONAL PHYSICS 70, 284–294 (1987)

Thomas–Fermi Equation with Non-spherical Boundary Conditions

M. FRIEDMAN

Department of Physics, NRCN, Beer-Sheva, Israel

A. RABINOVITCH

Department of Physics, Ben-Gurion University, Beer-Sheva, Israel

Y. ROSENFELD

Department of Physics, NRCN, Beer-Sheva, Israel

AND

R. THIEBERGER

Department of Physics, NRCN, Beer-Sheva, Israel and
Department of Physics, Ben-Gurion University, Beer-Sheva, Israel

Received April 25, 1986; revised August 5, 1986

The confined atom Thomas–Fermi equation with non-spherical boundary conditions is considered. A 2-D finite element code for solving the Thomas–Fermi equation with general boundary conditions is demonstrated. Results for both Dirichlet and Neumann boundary conditions for ellipsoids of revolution are presented. © 1987 Academic Press, Inc.

I. INTRODUCTION

A central feature in the Thomas–Fermi (TF) theory [1–5] for the equation of state (EOS) of elements at high densities is the "ion sphere" picture. In this theory, the properties of the bulk material are approximated by those of an isolated *spherically symmetric* "atom" of radius equal to the Wigner-Seitz radius, $a_{ws} = (3v/4\pi)^{1/3}$, where v is the volume per atom. Although founded by the notion of the Wigner-Seitz cell of a tightly packed periodic lattice, the ion sphere picture is introduced ad hoc.

We have several motivations for considering the confined atom TF problem with non-spherical boundary conditions. Many types of corrections to the basic TF approximation have been considered, including exchange, gradient, and nuclear motion effects. However, no systematic assessment is available of the relative importance of those corrections, in comparison with perturbations on the ad hoc spherical boundary conditions. Material subject to strong shocks may exhibit local deformations which may be better described by, say, ellipsoidal boundary con-

0021-9991/87 $3.00

ditions than by the customary spherical ones. For the spherical atom the Dirichlet and Neumann boundary conditions coincide. However, in the non-spherical case, these two sets of boundary conditions represent completely different assumptions about the nature of the bulk material. Dirichlet boundary conditions correspond to a conducting medium, and the isolation of the non-spherical neutral atom is obtained with the "aid" of the induced surface charge. For Neumann boundary conditions the isolation is obtained with the aid of a surface dipole layer. It is of both physical and mathematical interest to analyze, within the TF approximation, these different views of the bulk material and see how they merge for the spherical case.

Loughlin [6], solved the temperature-dependent equation for a spherical cell with a non-central nucleus, employing Neumann boundary conditions. He used this cell model for nuclear motion effects to study the temperature dependence of interatomic forces of normal-density matter and its effect on the equation of state.

Our intention, however, is to study the TF cell model with nonspherical boundaries. Very recent analysis [7] revealed that the electrostatic Poisson equation with Dirichlet boundary conditions is intimately connected to the integral equation theory of charged particles. Both the ion-sphere boundary condition and the picture of the bulk (electrons and ions) material as an infinite conductor, were shown to be contained within the theory of classical liquids in the hypernetted chain (HNC) approximation.

The high density solution of the HNC equations for charge-clusters plasmas, as met in the Onsager charge-smearing optimization, defines Onsager-TF-confined "molecules" [8]. These are natural generalizations of the TF-confined "atoms." The difference between the free energies of one such diatomic-molecule, and two separate atoms, as a function of the interatomic distance, r, in the molecule, is related to the nuclear pair correlation function, $g(r)$. These new developments provide further motivation to consider the TF-cell model with non-spherical boundaries.

Notwithstanding all of these motivations, the purpose of the present communication is mainly to outline the main points introduced by the deviations from spherical symmetry and develop a suitable numerical scheme.

The computational procedure used throughout this work was based on a finite element package, extended and modified to treat the nonlinearities of the TF type. The TF problem discussed in this paper enjoyed cylindrical symmetry and was solved over various ellipsoids of revolution. The authors' purpose, however, is to design a numerical tool that can be used for cases which do not necessarily possess cylindrical symmetry. Thus, a finite element approach was chosen rather than other methods; e.g., the Fourier–Bessel expansion which is often used in the related Grad–Shafranov equation of magneto-hydrodynamics [9].

In Section II the problem is formulated for general boundaries and boundary conditions. The numerical procedure for axisymmetric shapes is given in Section III. Results for both Dirichlet and Neumann boundary conditions for ellipsoids of revolution are presented in Section IV.

II. Thomas–Fermi Equation and the Virial Theorem

The TF theory supplements the atom confinement condition by the *statistical assumption*, which introduces free-electron-gas statistics *locally* within the atom: Let $\rho = F(\mu)$ be the ideal free-electron-gas relation between the chemical potential μ, and the electron density ρ. If $\varphi(\mathbf{r})$ is the electrostatic potential of a point $\mathbf{r}$ inside the confined atom with an ion of charge Ze at the origin, and $\rho(\mathbf{r})$ is the corresponding local electron density, then the TF relation is

$$\rho(\mathbf{r}) = F(\mu + e\varphi(\mathbf{r})). \tag{1}$$

Measuring distances in units of $\gamma = (9\pi^2/128Z)^{1/3}\, a_0$, where a_0 is the Bohr radius, and energies in units of Ze^2/γ, we let

$$\begin{aligned} \alpha &= Z/4\pi \\ r &= |\mathbf{r}| \\ \frac{\psi(\mathbf{r})}{r} &= \mu + e\varphi(\mathbf{r}) \end{aligned} \tag{2}$$

and obtain from (1) the zero temperature relation

$$\rho(\mathbf{r}) = \alpha \left(\frac{\psi}{r}\right)^{3/2}. \tag{3}$$

Bearing in mind the scaling properties of the model we take hereafter $Z = 1$, i.e., $\alpha = 1/4\pi$.

Using Poisson's equation of electrostatics, one gets the standard zero temperature TF equation

$$\nabla^2\psi(\mathbf{r}) = \psi^{3/2}(\mathbf{r})/r^{1/2} \tag{4}$$

with the central "boundary" condition

$$\psi(0) = 1. \tag{5}$$

For the spherically symmetric TF problem of an atom confined within a sphere of radius R, both Neumann

$$\nabla\varphi(\mathbf{r})\Big|_{\text{surface}} \cdot \hat{n} = \frac{\partial\varphi}{\partial n} = 0 \Rightarrow \frac{d\psi}{dr} = \frac{\psi}{r}\Big|_{r=R} \tag{6}$$

and Dirichlet

$$\varphi|_{\text{surface}} = 0 \underset{\text{sphere}}{\Rightarrow} \psi(R) = R\mu \tag{7}$$

boundary conditions coincide ($\hat{n}$ denotes the outward normal unit vector).

The charge neutrality condition

$$\alpha \int_v \left(\frac{\psi(\mathbf{r})}{r}\right)^{3/2} d^3r = 1 \tag{8}$$

needs to be imposed for a Dirichlet problem, while it is automatically satisfied in the Neumann case.

Only the combination $\mu + e\varphi(\mathbf{r})$ enters the Neumann problem and in order to determine μ, i.e., the thermodynamics, an additional constraint needs to be imposed (see below).

Given the solution of (4), (5), and (6) or (7), we may obtain the kinetic energy via

$$U_k = \frac{3}{5}\int_v \left(\frac{\rho(\mathbf{r})}{\alpha}\right)^{2/3} \rho(\mathbf{r})\, d^3r = \frac{3}{5}\alpha \int_v \left(\frac{\psi(\mathbf{r})}{r}\right)^{5/2} d^3r. \tag{9}$$

The potential energy is measured relative to the infinite self energy of the ion, U_{ii}, and is given by

$$U_P = \frac{1}{8\pi}\int_v \mathbf{E}\cdot\mathbf{E}\, d^3r - U_{ii}, \tag{10}$$

where $\mathbf{E}(\mathbf{r}) = -\nabla\varphi(\mathbf{r})$ is the electric field. On the other hand the potential energy U_p consists of the following electrostatic interactions: ion–electron U_{ie}, ion–surface charge U_{is}, electron–electron U_{ee}, electron–surface U_{es}, and surface–surface U_{ss},

$$U_P = U_{ie} + U_{ee} + U_{es} + U_{is} + U_{ss} \equiv U_P^{(0)} + U_{is} + U_{ss} + \tfrac{1}{2}U_{es}, \tag{11}$$

where

$$U_P^{(0)} = -\frac{5}{6}U_k + \frac{1}{2}\mu - \frac{1}{2}\alpha\int_v \frac{\psi(\mathbf{r})}{r^{5/2}}\, d^3r$$

is the usual expression for the potential energy in the spherical case. For the Neumann problem μ is still to be determined (see Eq. (20)), while for the Dirichlet problem we obtain

$$U_P = U_P^{(0)} - \frac{1}{8\pi}\int_s \frac{\mathbf{E}\cdot d\mathbf{s}}{r} \equiv U_P^{(0)} - I_2, \tag{12}$$

where I_2 (spherical) $= 0$, and s is the surface of v.

From the TF expression (3) and straightforward electrostatics using the identities given by More [10], we obtain the ("virial") identity

$$2U_k + U_P = \frac{2}{5}\int_s \left(\frac{\psi(\mathbf{r})}{r}\right)^{5/2} \mathbf{r}\cdot d\mathbf{s} + I_1, \tag{13}$$

where I_1, the electric field pressure is given by

$$I_1 = \pm\frac{1}{8\pi}\int_s |\mathbf{E}|^2\,\mathbf{r}\cdot d\mathbf{s}. \tag{14}$$

The signs $(+)$ and $(-)$ correspond to the Neumann and Dirichlet boundary conditions, respectively. For a sphere, $I_1 = 0$ and Eq. (13) takes the familiar virial-theorem form

$$2U_k + U_P = \tfrac{2}{5}\alpha\mu^{5/2}\cdot 3v \equiv p\cdot 3v, \tag{15}$$

where p is the pressure and v is the atomic volume. In view of the general scale analysis of Feynman, Metropolis and Teller [1], Eq. (13) should be interpreted as the virial theorem

$$3pv = \frac{2}{5}\int_s \left(\frac{\psi(\mathbf{r})}{r}\right)^{5/2}\mathbf{r}\cdot d\mathbf{s} + I_1. \tag{16}$$

Indeed, considering the free energy functional

$$\Omega[\psi] = U_k[\psi] + U_P[\psi] - \mu\alpha\int_v \left(\frac{\psi(\mathbf{r})}{r}\right)^{3/2} d^3r \tag{17}$$

and taking the volume derivative at constant ψ and shape, we obtain for the Dirichlet problem

$$\left(-\frac{\partial\Omega}{\partial v}\right) 3v = 2U_K + U_P. \tag{18}$$

Note that the pressure p is defined by Eqs. (15) and (16) which are otherwise obtained by plain electrostatics. Although this definition is not unique, it is the one usually adopted [10]. What singles it out as an appropriate definition of a pressure for the cell model of matter, is, that it obeys thermodynamic consistency. We thus impose the thermodynamic consistency $p = -\partial\Omega/\partial v$ for the Neumann condition as well, and find that it holds, provided that

$$\int_s \rho(\mathbf{r})\, e\varphi(\mathbf{r})\,\mathbf{r}\cdot d\mathbf{s} = -\frac{1}{4\pi}\int_s |\mathbf{E}|^2\,\mathbf{r}\cdot d\mathbf{s} \tag{19}$$

which in our units ($\alpha = 1/4\pi$) reads

$$\mu = \left(\int_s \left(\frac{\psi(\mathbf{r})}{r}\right)^{5/2}\mathbf{r}\cdot d\mathbf{s} + \int_s |\mathbf{E}|^2\,\mathbf{r}\cdot d\mathbf{s}\right) \Big/ \int_s \left(\frac{\psi(\mathbf{r})}{r}\right)^{3/2}\mathbf{r}\cdot d\mathbf{s}. \tag{20}$$

III. The Finite Element Scheme

The computations were performed using a 2-D finite element package MANFEP [11], that was extended and modified to treat the non-linear term of the TF type (Eq. (4)). The MANFEP code has already proved useful in solving various physical problems [12–14]. The new version processed the TF functional (Eq. 26) and established a respective system of non-linear equations, for which an initial guess had to be found. The appropriate 1-D problem was then solved (Appendix 1) for the same radius using overrelaxation factor extremely close to 2 to ensure fast convergence. This 1–D solution provided a first approximation for the 3-D ellipsoid.

Due to axial symmetry and using spherical coordinates, Eq. (4) takes the form

$$\psi_{rr}+\frac{1}{r^2\sin\theta}\frac{\partial}{\partial\theta}\left(\sin\theta\frac{\partial\psi}{\partial\theta}\right)-\frac{\psi^{3/2}}{\sqrt{r}}=0. \tag{21}$$

Furthermore, by defining

$$\begin{aligned} x&=r\sin\theta\\ y&=r\cos\theta \end{aligned} \tag{22}$$

one obtains

$$\psi_{xx}+\psi_{yy}+\frac{y^2-x^2}{x(x^2+y^2)}\psi_x-\frac{2y}{x^2+y^2}\psi_y-\frac{\psi^{3/2}}{\sqrt{x^2+y^2}}=0. \tag{23}$$

Consider an ellipsoid of revolution

$$D\equiv\left\{(x,y,z)\,\middle|\,\frac{x^2}{a^2}+\frac{y^2}{b^2}+\frac{z^2}{a^2}\leqslant 1\right\} \tag{24}$$

whose volume $\frac{4}{3}\pi a^2 b$ equals to that of a sphere with radius R, i.e., $a=R\eta$, $b=R/\eta^2$. The computations are then restricted to the first quarter of an ellipse in the $x-y$ plane. As mentioned before we distinguish between two cases.

a. *A Dirichlet Problem*

The boundary conditions are

$$\begin{aligned} &\psi(0,0)=1\\ &\psi(x,y)=r\mu, \qquad (x,y)\in C \end{aligned} \tag{25a}$$

$$\frac{\partial\psi(x,0)}{\partial n}=\frac{\partial\psi(0,y)}{\partial n}=0, \qquad 0\leqslant x\leqslant a,\ 0\leqslant y\leqslant b, \tag{25b}$$

where C is the ellipse's boundary. The constant μ is determined by the electro-neutrality condition (Eq. (8)). Equations (23), (25a), (25b) are solved by minimizing the functional

$$F(\psi)=\iint_{D'}\left[\frac{x}{y^2}(\psi_x^2+\psi_y^2)+\frac{4x\psi^{5/2}}{5r^{5/2}}\right]dx\,dy \tag{26}$$

over the set $\{\psi \mid \psi \in C^2(D'),\ \psi$ satisfies Eq. (25a)$\}$, where

$$D'=\left\{(x,y)\left|\frac{x^2}{a^2}+\frac{y^2}{b^2}\leqslant 1,\ x\geqslant 0,\ y\geqslant 0\right.\right\}. \tag{28}$$

Equation (25b) is then automatically satisfied being a natural boundary condition of the functional.

b. *A Neumann Problem*

The boundary conditions are

$$\begin{aligned}\psi(0,0)&=1\\ r\frac{\partial\psi}{\partial n}-\frac{\partial r}{\partial n}\psi&=0,\qquad \mathbf{r}\in C,\end{aligned} \tag{29}$$

and if one restricts computations to the first quarter, one should assume Eq. (25b) as well. The functional to be minimized for a Neumann problem is

$$F(\psi)=\iint_{D'}\left[\frac{x}{r^2}(\psi_x^2+\psi_y^2)+\frac{4x}{5r^{5/2}}\right]dx\,dy+\oint_C\frac{xr_n}{r^3}\psi^2\,ds. \tag{30}$$

While when solving a Neumann problem, MANFEP is called just once, a Dirichlet problem must be solved iteratively as follows: Given an ellipsoid of revolution D and any constant potential boundary condition μ, let

$$h(\mu)=\alpha\int_D\left(\frac{\psi_\mu}{r}\right)^{3/2}d^3r-1. \tag{31}$$

The electro-neutrality condition is $h(\mu)=0$ and is satisfied by some μ^*. Since for the spherical case the Neumann and Dirichlet problems are identical, one may first solve a spherical Neumann Problem (Appendix) and use its μ as a first approximation to μ^*. A Regula Falsi scheme is then applied to iteratively calculate μ^*.

IV. Results

We solved Eq. (23) for both Dirichlet and Neumann cases and for $R=1.19$, 2.8, 5.85. The values of $\mu=\psi(R)/R$ computed for the 1 – D Neumann problem (Appen-

TABLE I

A Dirichlet Problem

R	η	μ	U_K	$U_P^{(0)}$	I_1	I_2	p
1.19	1.0	1.220	1.365	−1.632	0.0002	0.0048	0.0523
1.19	1.2	1.248	1.361	−1.599	0.0599	0.0321	0.0526
1.19	0.8	1.250	1.367	−1.601	0.0631	0.0375	0.0526
2.80	1.0	0.172	0.738	−1.380	0	0.0015	0.00039
2.80	1.2	0.179	0.742	−1.377	0.0129	0.0112	0.00038
2.80	0.8	0.181	0.732	−1.361	0.0120	0.0108	0.00040
5.85	1.0	0.0263	0.657	−1.322	0.0001	0.0023	3.6×10^{-6}
5.85	1.2	0.0282	0.657	−1.319	0.0019	0.0045	3.5×10^{-6}
5.85	0.8	0.0288	0.649	−1.307	0.0019	0.0045	3.7×10^{-6}

dix) were in 5-digit agreement with previous results [2] and served as first approximations for μ^* of the nonspherical Dirichlet problems. They have also been used to solve 3-D spherical Dirichlet problems via MANFEP, enabling us to determine an accuracy rate of the results $\sim 0.5\%$ for ψ.

For each of the radii the TF equation was completely solved for $\eta = 0.8, 1, 1.2$. Tables I and II consist of the computed values of μ, U_k, $U_P^{(0)}$, I_1, I_2, and p for the Dirichlet and Neumann cases, respectively. The electron density distribution along the x, y axes is given in Fig. 1 and the normal and tangential electric field on the boundary for the Dirichlet and the Neumann problems respectively are given in Fig. 2. A typical finite element mesh (14 elements, 4th order polynomial approximations, 133 nodes) used in the computations is given in Fig. 3.

The accuracy of the numerical procedure can be estimated by comparing the "Dirichlet" and the "Neumann" results (Tables I, II) for the spherical case ($\eta = 1$). We observe that the pressure p is minimal for the sphere and that 20–25% asymmetry yields about 3% increase in the pressure.

TABLE II

A Neumann Problem

R	η	μ	U_K	$U_P^{(0)}$	I_1	I_2	p
1.19	1.0	1.210	1.350	−1.618	0.0004	0.0092	0.0511
1.19	1.2	1.269	1.365	−1.600	0.0644	0.0101	0.0531
1.19	0.8	1.313	1.388	−1.605	0.0895	0.0097	0.0549
2.80	1.0	0.169	0.736	−1.377	0.0001	0.0032	0.00038
2.80	1.2	0.190	0.748	−1.383	0.0106	0.0030	0.00042
2.80	0.8	0.196	0.731	−1.359	0.0116	0.0027	0.00042
5.85	1.0	0.0255	0.657	−1.321	0.0002	0.0032	3.2×10^{-6}
5.85	1.2	0.0486	0.659	−1.313	0.0074	0.0013	7.0×10^{-6}
5.85	0.8	0.0348	0.650	−1.306	0.0022	0.0033	4.7×10^{-6}

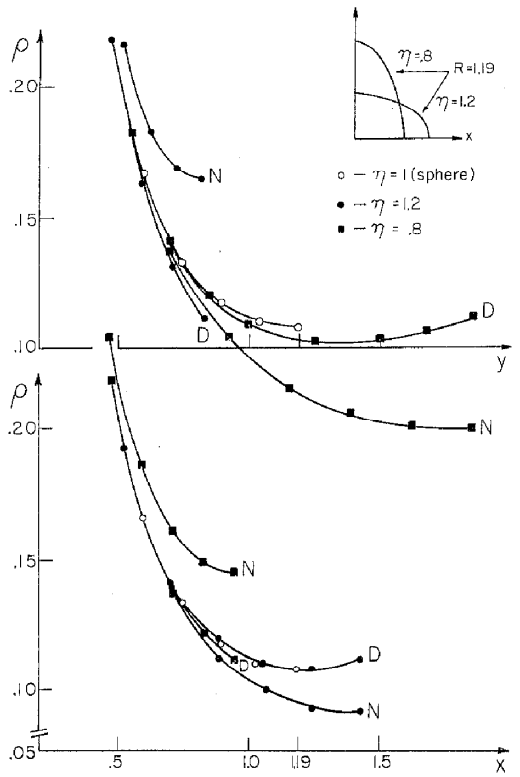

FIG. 1. Electron density along the axes for $R = 1.19$ and different asymmetries. N and D denote the Neumann and Dirichlet results, respectively.

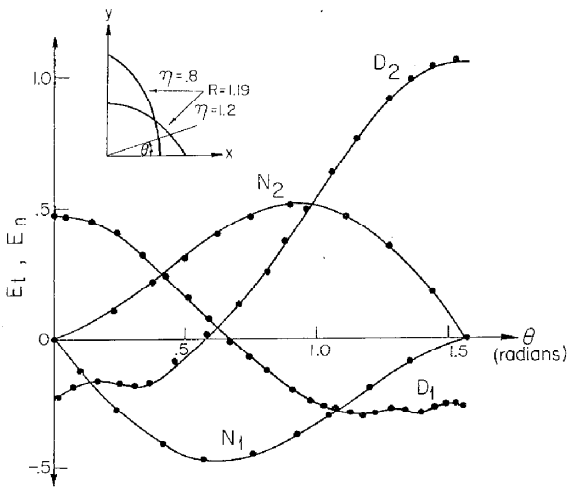

FIG. 2. Normal (E_n) and tangential (E_t) electric fields on the boundary for $R = 1.19$ as functions of the azimutal angle θ (in radians). N1 and N2 denote the tangential field for the Neumann case with $\eta = 0.8$ and $\eta = 1.2$, respectively. D1 and D2 denote the normal field for the Dirichlet case with $\eta = 0.8$ and $\eta = 1.2$, respectively.

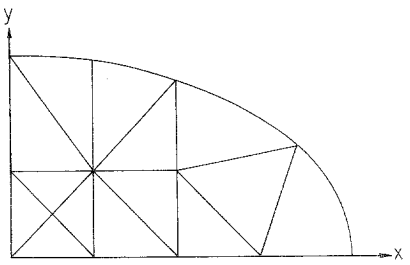

FIG. 3. A typical finite element mesh used in the computations.

We expect that the achieved accuracy in ψ will enable us to use the method for 2-D problems with general boundary conditions and shapes not necessarily with cylindrical symmetry. This is an advantage compared to a solution based on series expansions, where each case needs to be studied separately for its accuracy.

APPENDIX

The spherical TF Neumann problem consists of solving the 1-D equation

$$\nabla\psi = \psi^{3/2}/r^{1/2}, \qquad 0 \leqslant r \leqslant R \tag{A1}$$

with boundary conditions

$$\psi(0) = 1 \tag{A2}$$

$$R\left.\frac{\partial\psi}{\partial r}\right|_R - \psi(R) = 0. \tag{A3}$$

The interval $[0, R]$ is uniformly divided by grid points $0 = r_0 < r_1 < \cdots < r_n = R$ with $h = r_{i+1} - r_i$. At each internal point r_i, Eq. (A1) is replaced by its central finite differences equivalent—leading to

$$\psi_i = \frac{\psi_{i-1} + \psi_{i+1}}{2 + h^2(\psi_i r_i)^{1/2}}. \tag{A4}$$

The boundary condition (A3) is replaced by

$$\psi_n = \frac{(4 + 2h/R)\,\psi_{n-1} - \psi_{n-2}}{3} \tag{A5}$$

and Eqs. (A4)–(A5) are iterated using overrelaxation technique, until the difference between two consecutive iterations is less than a given tolerance.

REFERENCES

1. R. P. FEYNMAN, N. METROPOLIS, AND E. TELLER, *Phys. Rev.* **75**, 1561 (1949).
2. R. LATTER, *J. Chem. Phys.* **24**, 280 (1956).
3. N. H. MARCH, *Advan. in Phys.* **6**, 1 (1957).
4. S. G. BRUSH, "Theories of the Equation of State of Matter at High Pressures and Temperatures," in *Progress in High Temperature Physics and Chemistry*, edited by C. A. Rouse (Pergamon, Oxford, 1967), Vol. 1, p. 1.
5. R. M. MORE, "Atomic Physics in Inertial Confinement Fusion," Lawrence Livermore Nat'l Laboratory Report No. UCRL-84991, 1981 (unpublished).
6. R. B. LAUGHLIN, *Phys. Rev. A* **33**, 510 (1986).
7. Y. ROSENFELD, *Phys. Rev. A* **32**, 1834 (1985); **33**, 2025 (1986); Y. ROSENFELD AND L. BLUM, *J. Phys. Chem.* **89**, 5149 (1985); *J. Chem. Phys.* **85**, 1556 (1986).
8. Y. ROSENFELD, *Phy. Rev. A*, in press.
9. G. BATEMAN *MHD Instabilities* (MIT Press, Cambridge, MA, 1978).
10. R. M. MORE, *Phys. Rev. A* **19**, 1234 (1979).
11. M. FRIEDMAN, D. J. RICHARDS, W. N. R. STEVENS, AND A. WAXLER, "MANFEP;" University of Manitoba Finite Element Program, Department of Electrical Engineering, University of Manitoba, Winnipeg, Man. R3T 2N2, Canada, 1979 (unpublished).
12. M. FRIEDMAN, Y. ROSENFELD, A. RABINOVITCH, AND R. THIEBERGER, *J. Comput. Phys.* **26**, 169 (1978).
13. M. FRIEDMAN, A. RABINOVITCH AND R. THIEBERGER, *Z. Phys. A* **316**, 1(1984).
14. R. AVIDA, J. YEHESKEL, M. FRIEDMAN, D. GAZIT, AND D. LEVRON, *Rev. Sci. Instrum.* **53**, 1577 (1982).